

## Passivation of n and p dopants in ion-implanted GaAs by a 2D+ plasma

D. K. Sadana, J. P. de Souza, E. D. Marshall, H. Baratte, and F. Cardone

Citation: *Applied Physics Letters* **58**, 385 (1991); doi: 10.1063/1.104642

View online: <http://dx.doi.org/10.1063/1.104642>

View Table of Contents: <http://scitation.aip.org/content/aip/journal/apl/58/4?ver=pdfcov>

Published by the [AIP Publishing](#)

---

### Articles you may be interested in

[Nuclear radiation detectors based on a matrix of ion-implanted p-i-n diodes on undoped GaAs epilayers](#)  
*AIP Conf. Proc.* **1496**, 50 (2012); 10.1063/1.4766487

[Correlation between electronegativity and dopant activity in ion-implanted semi-insulating GaAs](#)  
*Appl. Phys. Lett.* **57**, 378 (1990); 10.1063/1.103697

[Electroreflectance of ion-implanted GaAs](#)  
*J. Appl. Phys.* **52**, 2950 (1981); 10.1063/1.329035

[Ion-implanted Se in GaAs](#)  
*J. Appl. Phys.* **51**, 4130 (1980); 10.1063/1.328232

[Close-contact annealing of ion-implanted GaAs and InP](#)  
*Appl. Phys. Lett.* **36**, 927 (1980); 10.1063/1.91376

---

A promotional banner for Applied Physics Reviews. On the left is a cover image of the journal showing a diagram of a device structure. The main text reads 'NEW Special Topic Sections' in large white letters on a blue background. Below this, it says 'NOW ONLINE' in yellow, followed by 'Lithium Niobate Properties and Applications: Reviews of Emerging Trends' in white. The AIP Applied Physics Reviews logo is in the bottom right corner.

**NEW Special Topic Sections**

**NOW ONLINE**  
Lithium Niobate Properties and Applications:  
Reviews of Emerging Trends

**AIP** Applied Physics  
Reviews

# Passivation of $n$ and $p$ dopants in ion-implanted GaAs by a $^2\text{D}^+$ plasma

D. K. Sadana, J. P. de Souza,<sup>a)</sup> E. D. Marshall, H. Baratte, and F. Cardone  
IBM T. J. Watson Research Center, Yorktown Heights, New York 10598

(Received 23 July 1990; accepted for publication 30 October 1990)

Strong  $n$  but weak  $p$ -carrier passivation was observed when Si- and Mg-implanted/annealed GaAs samples were exposed to a  $^2\text{D}$  plasma under identical conditions. Even though a discrete band of dislocation loops was present in both the samples, the  $^2\text{D}$  distribution in the two cases was remarkably different. In the Si-implanted sample the  $^2\text{D}$  followed the carrier distribution, whereas in the Mg-implanted sample it followed the distribution of dislocation loops. Phenomenological mechanisms of  $^2\text{D}$  interaction with dopants/dislocations in GaAs are postulated.

Fabrication of semiconductor integrated circuits routinely utilizes plasma-enhanced chemical vapor deposition (PECVD) of  $\text{SiO}_2$  and  $\text{Si}_3\text{N}_4$  films on the surface of the semiconductor. However,  $\text{H}^+$  is created during the PECVD and semiconductors are inadvertently exposed to the atomic or ionized H until a continuous coverage of the film occurs on the semiconductor.<sup>1</sup> Both shallow acceptors as well as shallow donors are known to be passivated in GaAs after a H plasma exposure.<sup>2-5</sup> The published work on the H passivation in III-V semiconductors, however, is focused primarily on either the bulk-grown material or homo/hetero epitaxially grown material.<sup>2,3</sup> The H-damage interaction in GaAs has mainly been studied in  $\text{H}^+$ -implanted/annealed GaAs.<sup>6,7</sup> It is demonstrated here that H follows precisely the carrier distribution in GaAs when a Si-implanted/annealed GaAs sample is exposed to a H plasma. In the Mg-implanted/annealed GaAs there is no correspondence between the distributions of the  $p$  carriers and H.

Semi-insulating, liquid-encapsulated (100)GaAs wafers were implanted with  $^{29}\text{Si}$ , Mg, or Be. The implant conditions for each ion are described separately in the ensuing text. Some of the low dose ( $\approx 1 \times 10^{13} \text{ cm}^{-2}$ )  $\text{Si}^+$ -implanted samples were also co-implanted with  $\text{Mg}^+$  to create a buried  $p$  layer. A portion of each implanted sample subsequently underwent capless rapid thermally annealing (RTA) in a Heatpulse 410T Annealer at  $850^\circ\text{C}$  for 10 s. The capless RTA was performed in Ar or forming gas with the implanted side facing down on a Si wafer coated with a layer of  $\text{Si}_3\text{N}_4$ . The unannealed and annealed samples were then exposed to a  $^2\text{D}$  plasma in a Plasmatherm system at  $300^\circ\text{C}$  for 5 min. Deuterium instead of hydrogen was used for the plasma to improve the detection efficiency of H in GaAs by secondary-ion mass spectrometry (SIMS). Capacitance-voltage ( $C$ - $V$ ) and Hall measurements were performed on the annealed samples before and after the plasma treatment. The distribution of secondary defects was obtained on a selected number of samples by cross-sectional transmission electron microscopy (XTEM).

Figure 1 shows a set of carrier concentration versus depth profiles obtained by  $C$ - $V$  measurements from the

samples that were dual implanted with  $30 \text{ keV } ^{29}\text{Si}^+$  to a dose of  $6 \times 10^{12} \text{ cm}^{-2}$  and  $120 \text{ keV } \text{Mg}^+$  to doses of 0,  $1 \times 10^{11}$ ,  $3 \times 10^{11}$ , and  $10 \times 10^{11} \text{ cm}^{-2}$ , and subsequently capless annealed at  $850^\circ\text{C}/10 \text{ s}$ . It is evident that the carrier compensation increases systematically in the tail with the increasing dose of the Mg.

After the  $C$ - $V$  measurements, the samples of Fig. 1 were exposed to a  $^2\text{D}$  plasma in a manner already described above. The carriers were found to be totally passivated after the plasma treatment. Neither Hall nor  $C$ - $V$  measurements could be performed on the samples. The passivation correlated with the fast diffusion of the  $^2\text{D}$  into the implanted region of the GaAs. Figure 2 shows the SIMS-measured  $^2\text{D}$  distributions in the samples of Fig. 1. It is remarkable that the  $^2\text{D}$  distributions followed precisely the carrier distributions of Fig. 1 in its magnitude as well as in the shape. Even the different levels of tail compensation in Fig. 1 were reflected in the  $^2\text{D}$  profiles. Although the carrier compensation by H in the previous work<sup>1-4</sup> was correlated with the diffusion of H during a H plasma treatment, the exact correspondence between the carrier profiles and the diffused H profiles observed here is a new finding. The passivated carriers could be reactivated at a level of  $> 80\%$  after a heat treatment at  $350^\circ\text{C}$  for 10 min. The

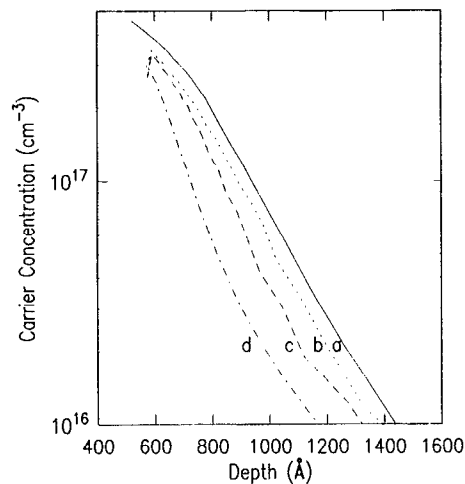


FIG. 1.  $C$ - $V$  measured carrier concentration profiles from the samples implanted with  $^{29}\text{Si}^+$  at  $30 \text{ keV}$  to a dose of  $6 \times 10^{12} \text{ cm}^{-2}$ . The co-implant doses of  $120 \text{ keV } \text{Mg}$  were (a) 0, (b)  $1 \times 10^{11} \text{ cm}^{-2}$ , (c)  $3 \times 10^{11} \text{ cm}^{-2}$ , and (d)  $10 \times 10^{11} \text{ cm}^{-2}$ . All samples underwent post-implant annealing at  $850^\circ\text{C}/10 \text{ s}$ .

<sup>a)</sup>Permanent address: Instituto de Física, UFRGS, 91500 Porto Alegre, RS Brazil.

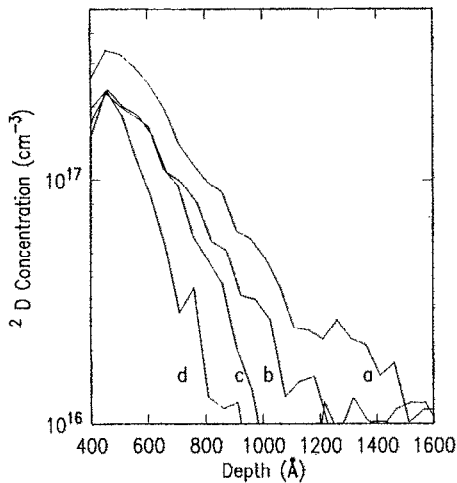


FIG. 2. SIMS measured  $^2\text{D}$  concentration profiles in the samples of Fig. 1. Note the remarkable similarity between the  $^2\text{D}$  and carrier profiles.

reactivation was accompanied by the outdiffusion of the H present in the implanted region. This point is illustrated again in Fig. 3.

The diffusion behavior of the  $^2\text{D}$  in GaAs implanted with a higher dose of  $\text{Si}^+$ , i.e.,  $4.5 \times 10^{13}$  or  $1 \times 10^{14} \text{ cm}^{-2}$  was also studied. The implant energy and subsequent RTA conditions were the same as used for the samples in Fig. 1. Figure 3(b) shows the profiles of the  $^2\text{D}$  in the sample after

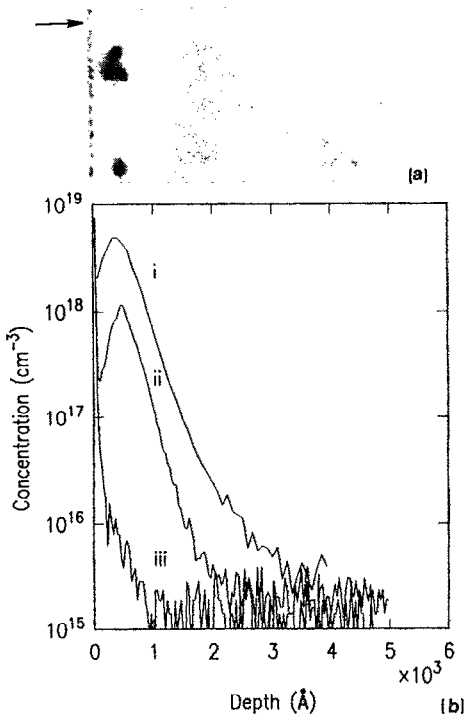


FIG. 3. GaAs sample implanted with  $^{29}\text{Si}$ , 30 keV,  $4.5 \times 10^{13} \text{ cm}^{-2}$  and subsequently annealed at  $850^\circ\text{C}/10 \text{ s}$ : (a) an XTEM micrograph showing the distribution of dislocation loops, (b) the corresponding SIMS profiles of  $^{29}\text{Si}$  (i) and  $^2\text{D}$  (ii) from the sample, and  $^2\text{D}$  profile after a  $350^\circ\text{C}/10 \text{ min}$  anneal (iii).

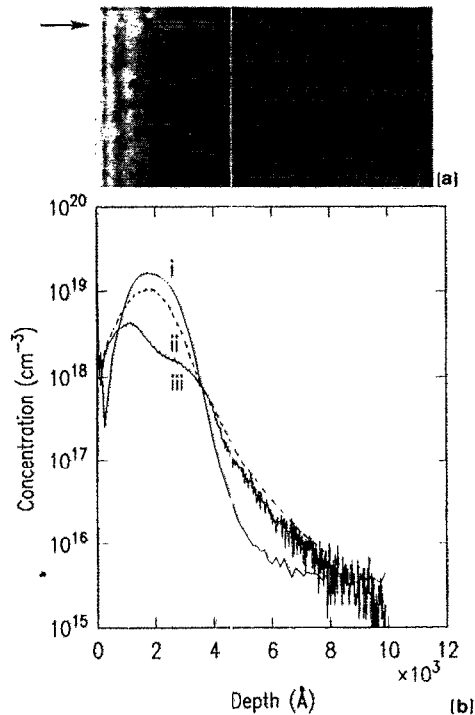


FIG. 4. GaAs sample implanted with Mg, 120 keV,  $1.0 \times 10^{14} \text{ cm}^{-2}$  and subsequently annealed at  $850^\circ\text{C}/10 \text{ s}$ : (a) an XTEM micrograph showing the distribution of dislocation loops and (b) the corresponding SIMS profiles of  $^2\text{D}$  (i) and Mg (iii) from the annealed sample. Also included in (b) is the Mg profile (ii) from the unannealed sample.

the plasma exposure. Also included in the figure is the profile of  $^{29}\text{Si}$  in the annealed sample. Since the implanted Si does not redistribute during the RTA, the Si profile for the unannealed sample is also the same as the annealed one included in Fig. 3(b). It is clear from Fig. 3(b) that the overall magnitude of the  $^2\text{D}$  is lower than that of the Si. The Hall data from this sample prior to the plasma treatment gave a peak carrier concentration of  $1\text{--}2 \times 10^{18} \text{ cm}^{-3}$ . As was the case with low-dose Si-implanted samples of Fig. 1, the level of  $^2\text{D}$  in Fig. 3(b) in the peak region ( $1.5 \times 10^{18} \text{ cm}^{-3}$ ) correlates rather closely with the measured peak carrier concentration in the high-dose Si-implanted sample. Furthermore, the sample becomes totally passivated after the plasma treatment. Although differential Hall measurements were not conducted in this investigation, based on the magnitude of  $^2\text{D}$  in Fig. 3(b) and the data of Fig. 2, it is believed that the  $^2\text{D}$  distribution in Fig. 3(b) before heat treatment represents the carrier distribution in the sample. The outdiffusion behavior of  $^2\text{D}$  during a subsequent heat treatment at  $350^\circ\text{C}$  for 10 min was also similar to what was observed in Fig. 2. Again, the outdiffusion of the  $^2\text{D}$  was accompanied by reactivation ( $\sim 80\%$  of the value prior to the plasma exposure) of the Si in the implanted region.

$\text{Mg}^+$  and  $\text{Be}^+$ -implanted/annealed samples were also exposed to a  $^2\text{D}$  plasma under the same conditions as were used for the samples of Figs. 2 and 3. Figure 4 shows the  $^2\text{D}$  profile in the  $\text{Mg}^+$ -implanted/annealed sample along with the Mg profiles before and after capless RTA at

850 °C/10 s. Unlike Si, a pronounced redistribution of Mg occurs after the annealing in high-dose Mg samples.<sup>8,9</sup> In fact, a significant fraction (20%) of the implanted Mg is found to outdiffuse during the annealing. It has been shown previously that the Mg retained in the GaAs after the annealing is nearly 100% electrically active.<sup>8</sup> It implies that the carrier profile in the annealed sample should be identical to the Mg profile. However, the <sup>2</sup>D distribution in Fig. 4 has no resemblance to the Mg distribution in the annealed sample. The <sup>2</sup>D profile is Gaussian in shape and the overall magnitude of the <sup>2</sup>D is higher than that of the Mg. Furthermore, a post-plasma anneal even up to 850 °C/10 s does not cause any significant outdiffusion of the <sup>2</sup>D. Despite the high concentration of <sup>2</sup>D in the implanted region, carrier passivation of only 20% occurred in the Mg- or Be-implanted sample. In contrast, under the identical <sup>2</sup>D plasma conditions the Si-implanted samples showed 100% carrier passivation. The XTEM micrographs [Figs. 3(a) and 4(a)] revealed that both samples contain dislocation loops and the mean depth of the loops correspond closely to the projected range of the implanted ion. It should be noted that the peak of the displacement damage distribution does not generally coincide with that of the implanted ion. However, in the present case the difference between the ion and damage distributions is within the uncertainty of the XTEM measurements. Comparison of Figs. 4(a) and 4(b) also shows that the depth distribution of <sup>2</sup>D in the Mg-implanted sample correlates precisely with the depth distribution of the dislocation loops in the sample. Similar findings were confirmed in the Be-implanted/annealed samples (not included). However, in the case of the Si-implanted samples the effect of the dislocation loops on the diffusion of the <sup>2</sup>D during the plasma exposure is not discernible, because the depth distributions of the carriers and dislocation loops overlap in Fig. 3. However, based on the electrical compensation data of Fig. 2 and the comparable levels of <sup>2</sup>D and carrier density in the sample of Fig. 3, it seems that the dislocation loops play only a minor role in affecting the <sup>2</sup>D diffusion in the sample.

The reason for the weaker carrier passivation in *p*-implanted samples observed in this investigation is not so straightforward. Since holes have an inherent tendency of recombining with electrons, they should also be strong capturing sites for the atomic H which has an unsaturated 1s orbit with one electron. However, a close examination at the <sup>2</sup>D binding to donors and acceptors in GaAs shows that the local atomic configurations in the two cases can be significantly different. For example, in the case of *n* dopants, the “free” electrons are in fact loosely bound to donors with an atomic radius of 100–200 Å with a hydrogen-like bonding. It is postulated that the passivation occurs when a “free” electron of the Si is intercepted by a 1s electron of the diffused H to form a weak Si-H bond. The bond length in this configuration could be of the order of the radius of the “free” electron and the bond would not be localized with respect to the donor atom. The crystal presumably can accommodate the bound H on a nonsubstitutional site. However, holes in a semiconductor are localized because they are tightly bound with acceptors. The passi-

vation of a hole requires the 1s electron of the H to recombine with the hole. The H therefore becomes localized with respect to an acceptor atom based on this model. Thus, in the case of Mg the hole passivation would require the formation of a tightly bound Mg-H-As type configuration. It appears intuitively that such an atomic configuration would not be energetically favorable and may be the cause of the weak passivation observed in the case of *p* dopants. The model proposed here is quite speculative at present.

The anomalous <sup>2</sup>D-dislocations interaction in Si- and Mg- or Be-implanted GaAs observed here is also a new phenomenon and is not documented in the literature. The two orders of magnitude difference in <sup>2</sup>D segregation to seemingly similar types of dislocation loops in the Si- and Mg-implanted GaAs indicates that either the core of the dislocations is radically different in the two materials and/or it is related to different Fermi levels in the two materials. It has been demonstrated recently on plastically deformed bulk GaAs that the charge states of dislocations can be different depending on whether the GaAs is *n* or *p* type.<sup>10</sup> This could be an additional factor that needs to be taken into account to explain the discrepancy of the <sup>2</sup>D redistributions in Figs. 3(b) and 4(b).

In summary, it has been demonstrated that in the Mg-implanted/annealed GaAs the overall concentration of the <sup>2</sup>D in the implanted region is an order of magnitude higher compared to the Mg profile and the profile of the diffused <sup>2</sup>D correlates precisely with the damage profile. In the case of Si-implanted/annealed GaAs, on the other hand, the <sup>2</sup>D profile correlates with the carrier profile. Consequently, the overall concentration of the diffused <sup>2</sup>D depends on the implanted Si dose, and is never higher than the Si concentration. At low doses ( $\lesssim 1 \times 10^{13} \text{ cm}^{-2}$ ) where nearly 100% Si activation occurs upon subsequent annealing, the magnitude of the <sup>2</sup>D is equivalent to that of the Si. However, at high doses ( $\gtrsim 1 \times 10^{13} \text{ cm}^{-2}$ ) of Si, the magnitude of the diffused <sup>2</sup>D is less than that of the Si. Despite the higher concentration of the <sup>2</sup>D in the Mg-implanted GaAs compared to the Si-implanted GaAs, the carrier compensation is less pronounced in the former samples.

The authors are indebted to Harry Hovel for useful discussions. The technical help of Joe Mitchell, Thermon McKoy, Maurice Norcott, and Jonah Kaszovitz is gratefully acknowledged.

<sup>1</sup>J. P. de Souza, D. K. Sadana, H. Baratte, and F. Cardone, *Appl. Phys. Lett.* **57**, 1129 (1990).

<sup>2</sup>J. Chevallier, W. C. Dautremont-Smith, C. W. Tu, and S. J. Pearton, *Appl. Phys. Lett.* **47**, 108 (1985).

<sup>3</sup>N. M. Johnson, R. D. Burnham, R. A. Street, and R. L. Thornton, *Phys. Rev. B* **33**, 1102 (1986).

<sup>4</sup>S. Pearton, J. W. Corbett, and T. S. Shi, *Appl. Phys. A* **43**, 153 (1987).

<sup>5</sup>B. Pajot, *Proc. Mater. Res. Soc. (Boston)* **163**, 465 (1990).

<sup>6</sup>J. H. Neethling, H. C. Snyman, and C. A. B. Hall, *J. Appl. Phys.* **63**, 704 (1988).

<sup>7</sup>J. M. Zavada, R. G. Wilson, and S. W. Novak, *Proceedings of the 17th European Solid State Devices Research Conference (Bologna, Italy) (Amsterdam, North Holland, 1987)*, pp. 927–929.

<sup>8</sup>H. Baratte, T. N. Jackson, D. K. Sadana, J. F. Degelormo, G. J. Scilla, and F. Cardone, *Proc. Mater. Res. Soc. (Boston)* **144**, 451 (1989).

<sup>9</sup>H. Baratte, D. K. Sadana, J. P. de Souza, P. E. Hallali, R. G. Schad, M. Norcott, and F. Cardone, *J. Appl. Phys.* **67**, 6589 (1990).

<sup>10</sup>D. Ferre and J. L. Farvacque, *Rev. Phys. Appl.* **25**, 323 (1990).